INSTITUTE OF PHYSICS PUBLISHING JOURNAL OF PHYSICS: CONDENSED MATTER

J. Phys.: Condens. Matter **14** (2002) 857–864 PII: S0953-8984(02)27754-1

Small-angle x-ray scattering study of nanocrystalline Fe_yCu_{1-y} alloys produced by ball milling

M B Fernández van Raap[1], L M Socolovsky[1], F H Sánchez[1] and I L Torriani[2]

[1] Departamento de Física, Facultad de Ciencias Exactas, Universidad Nacional de La Plata, c.c. 67, 1900 La Plata, Argentina
[2] Instituto de Fisica, Unicamp CP 6165/CEP 13083-970, Campinas, Brazil

E-mail: raap@venus.fisica.unlp.edu.ar

Received 6 August 2001, in final form 23 November 2001
Published 18 January 2002
Online at stacks.iop.org/JPhysCM/14/857

Abstract

Small-angle x-ray scattering measurements on ball-milled Fe_yCu_{1-y} giant-magnetoresistive alloys ($0.141 \leqslant y \leqslant 0.45$) have been performed using synchrotron radiation. For samples with different nominal compositions, prepared under exactly the same conditions, the scattered intensity recorded as a function of the wavevector varied systematically. For this reason, the strong scattering signal was attributed mainly to composition fluctuations in the crystalline grains. The system was treated as a two-phase model consisting of Fe-rich regions in a homogeneous Cu matrix, with composition-dependent relative volume fractions. Real-space analysis of the scattering was performed in terms of a volumetric distribution of spherical particles. Results indicate that the main contribution corresponds to 2 nm scattering objects of well-defined density contrast. The invariant Q was calculated to assess the variations in electron-density contrast as a function of the Fe content in the samples. Calculations based on these results allowed the determination of 0.35 at.% iron concentration in the iron-rich phase for all the nominal compositions studied.

1. Introduction

Mechanical alloying is a technique widely used to synthesize different kinds of non-equilibrium phase such as amorphous, quasicrystalline and nanocrystalline phases [1]. Within such phases, formation of extended nanocrystalline solid solutions has frequently been observed in various alloy systems, including those having a miscibility gap. Whether or not compositional homogeneity is obtained by applying mechanical work to Fe–Cu systems is still an open question [2,3]. Moreover, to our knowledge, there has been no investigation of the particle size distribution and composition of iron-rich regions with varying composition in inhomogeneous FeCu alloys. For this system a giant-magnetoresistance (GMR) effect has been detected for iron

concentration between 5 and 45 at.%, with a maximum effect at 20 at.% Fe [4]. This negative change of the electric resistance of alloys placed in a magnetic field is obtained in granular alloys when a non-magnetic solvent (Cu) contains a magnetic solute (Fe) forming a heterogeneous solution [5]. The GMR effect was observed for the first time in FeAu alloys [6]. Later this subject attracted wide attention because new techniques designed for the production of tailored nanostructures allowed a controlled and systematic study of this phenomenon. In the case of condensation from the gas phase, magnetic particle size and distribution are easily controlled. However, in mechanically alloyed systems these features are unclear. We believe that low-resolution structural techniques like small-angle x-ray scattering (SAXS) using synchrotron radiation are very useful for studying these low-contrast systems and determining the size and shape parameters of these compositional inhomogeneities. For instance, a heterogeneous solution may correspond to any form of spatial composition fluctuation, including clusters and lamellar-type structures.

In this paper it is shown that the SAXS technique is probably the only one which can give direct information on cluster size and shape parameters in magnetoresistive Fe_yCu_{1-y} ($0.141 \leqslant y \leqslant 0.45$) alloys prepared by ball milling. The samples used in this SAXS study were taken from the same ball-milling batch as those used in the GMR experiments previously reported [4].

2. Experimental procedure

Powders of Fe (99.9% purity and 200 mesh) and Cu (99.9% purity and 300 mesh) were subjected to milling for 75 h in a water-refrigerated vibratory Nissin Gikken NEV-MA8 low-energy mill, under Ar atmosphere. The milling device was used at a working frequency of 13.3 Hz, with a stainless steel vial and a ratio of ball mass to powder mass of $C_r = 25$. The prepared stoichiometries were Fe_yCu_{1-y} with $y = 0.141$, 0.188, 0.25, 0.35 and 0.45. Details of the ball-milling technique used and of previous studies of these samples can be found elsewhere [4]. For the SAXS measurement, the powders were pressed in a sample holder having a 10 mm by 3 mm window of 0.4 mm thickness and wrapped with Kapton® tape.

Compaction under pressure was not performed, in order to avoid the formation of nano-pores, which would contribute to our SAXS pattern. The sample, as obtained from the ball-milling equipment, consists of powder particles of typically 1 μm size. A rough estimate of the pore diameters in the loose powder was obtained by calculating the free space between three 1 μm spherical particles: 360 nm, which is beyond our detection limits.

SAXS experiments were performed using synchrotron radiation at the SAXS beamline of the LNLS (National Synchrotron Light Laboratory), Campinas, Brazil. Details of the beamline optics can be found in [7]. Data were collected in transmission geometry with a linear position-sensitive detector placed at 1.5 and 0.6 m from the sample. These camera lengths correspond to scattering vectors $k = 4\pi(\sin\theta)/\lambda$ from 0.0052 to 0.2 Å^{-1} and from 0.2 to 0.45 Å^{-1} respectively, θ being half of the scattering angle. For the short camera length a wide beam-stop was placed in front of the detector in order to record only the $k > 0.2$ Å range, thus improving the counting detector efficiency. An incident wavelength $\lambda = 1.756$ Å, corresponding to a photon energy just below the Fe K-absorption edge, was chosen to avoid fluorescence. No mathematical desmearing was necessary because the x-ray spot over the sample was approximately 1 mm (vertical) × 5 mm (horizontal), the detection being performed in the vertical direction.

Normalization was achieved by dividing the data by $I_T h e^{-\mu x}$, where h is the detector response for each data point, μ the absorption coefficient, x the sample thickness and I_T

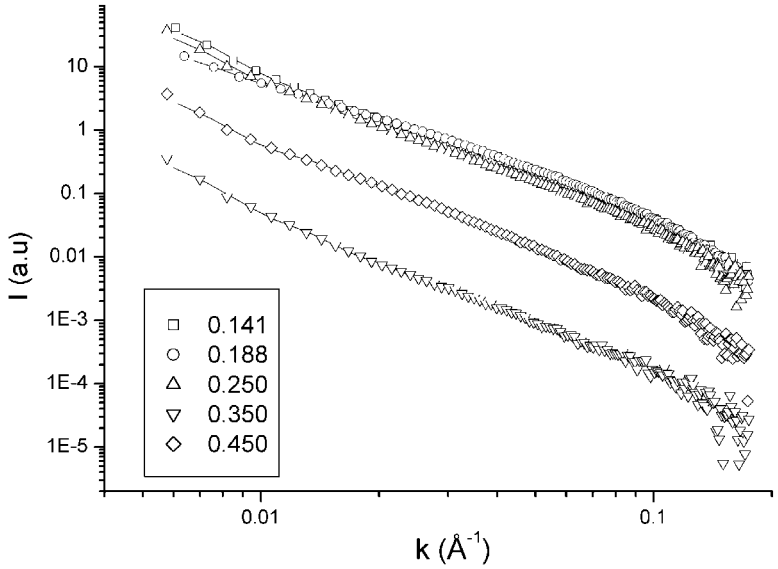

Figure 1. Scattering curves for Fe_yCu_{1-y} ($0.141 \leqslant y \leqslant 0.450$) obtained with a camera length of 1.5 m (square points). The fitted intensity calculated for a distribution of spheres is included (solid curve).

the integrated incident intensity recorded during the acquisition time t. Then, the data were corrected for parasitic scattering due to the air path in the sample holder and the Kapton® windows, by subtracting the scattering recorded from an empty sample holder under identical experimental conditions. The attenuation factor $e^{-\mu x}$ was determined by recording the beam intensity with two scintillation detectors placed in front of and behind the sample.

An important feature of the scattering is the apparent fall-off of the intensity with increasing scattering vector at large k (typically $k > 0.1$ Å). This is the region of the reciprocal space where the scattering from particle surfaces dominates. The $1/k^4$ power law is the characteristic Porod law for sharp interfaces and has been used to remove the constant, background contribution from incoherent sample scattering (e.g. fluorescence and resonant Raman scattering). Thus, a function of the type $A + B/k^4$ was fitted to the large-k regions ($0.1 < k < 0.20$ Å^{-1}) and the constant A subtracted from the data.

For the data acquired with the 0.6 m camera length, subtraction of parasitic scattering was not always possible due to the strong Kapton® peak at $k \sim 0.4$ Å^{-1} [8]. These data were only used to check whether the Porod region was well defined or any other feature appeared in the 0.2 Å $< k < 0.45$ Å range; see the inset in figure 2.

3. Results

The SAXS data for all the samples show the same smooth decreasing behaviour in the whole k-range studied here. The data are shown in figure 1 in a log–log plot; it can be noticed that the intensity decreases with Fe concentration up to $y = 0.35$. The k^{-4}-power law is shown for the $Fe_{0.141}Cu_{0.859}$ spectrum for 0.1 Å$^{-1} \leqslant k \leqslant 0.45$ Å^{-1} (figure 2). Although this Porod fit was not used for any numerical structural determination, the behaviour of the curves indicates the existence of sharp interfaces and suggests that the sample may be treated as a 3D particulate system.

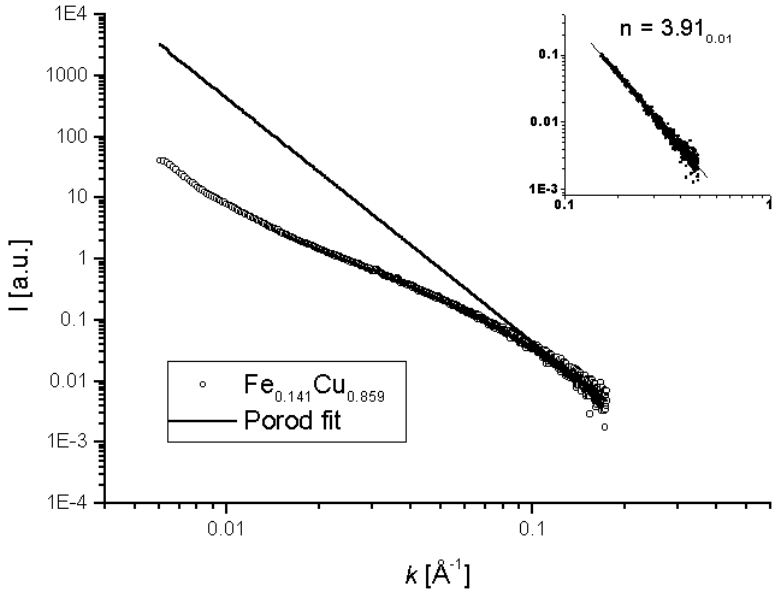

Figure 2. A log–log graph for $Fe_{0.141}Cu_{0.859}$. Inset: data obtained with a 0.6 m camera length and the Porod fit value $n = 3.91 \pm 0.01$ (no background subtraction).

Since the Porod law, characteristic of sharp interfaces, is obeyed, and the Guinier plots do not present a linear behaviour, the alloy is considered a system of polydisperse scattering objects distributed in a matrix. In this case, the scattered intensity function is related to a volumetric distribution of scattering centres $D_V(R)$ through the integral $I(k) = \int_0^\infty \langle F^2(kR)\rangle D_v(R)\,\mathrm{d}R$, where $\langle F(kR)\rangle$ is the mean scattering form factor which should be assumed known for determining $D_V(R)$. The GNOM program package due to Svergun (in 1992) [9] was used to fit a hypothetical volume size distribution function of spherical particles, defined as $D_V(R) = 4\pi R^3 N(R)/3$, where $N(R)$ is the relative number of spheres with radius between R and $R+\mathrm{d}R$. The assumption of a spherical form factor is a good assumption for concentrations no too close to $y = 0.5$ for which connection between inhomogeneities is expected. Results are shown in figure 3. It can be noticed that the main scattered intensity arises from particle radii smaller than $\sim$12 nm. The spread part of the distribution, for large sizes up to 45 nm, is a need to fit the low-k part of the scattering, which may be strongly connected to macroscopic sample imperfections such as surface irregularities and oxide layers [10].

Nanocrystalline solids produced by inert-gas condensation are obtained by high-pressure compaction of the isolated crystallites a few nanometres in diameter. In this case, the residual porosity and grain boundaries are on the same length scale [11, 12]. On the other hand, for nanocrystalline materials produced by ball milling, each powder particle is itself composed of nanometric crystallites. The crystallite sizes for our Fe–Cu system, as determined from XRD, are typically in the range 9–20 nm, these values being in agreement with previous results [13]. A high density of grain boundaries (typically 1 nm thick) is also present and voids may be present or not depending on the starting materials involved. Then, some scattering may arise from voids and/or the high density of grain boundaries usually present in nanocrystalline materials. In principle, this scattering cannot be separated from that coming from composition-density fluctuations inside the grains, but since all the samples were subjected to milling for the same time of 75 h, differences from one pattern to another are believed to be essentially due to

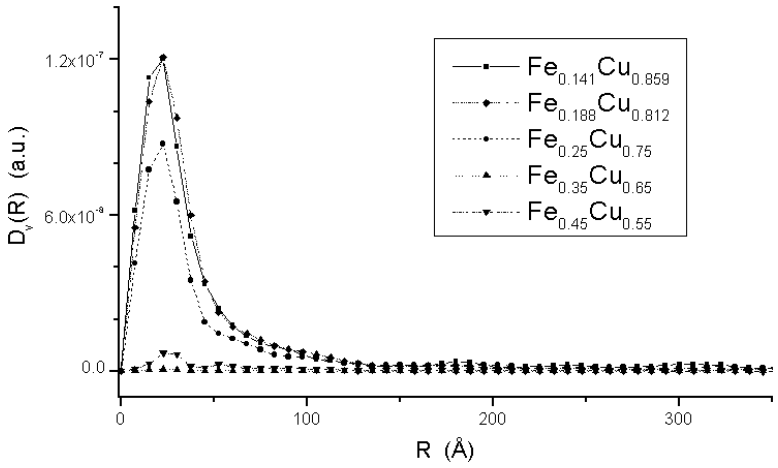

Figure 3. The size volumetric distribution function, assuming a spherical structure factor.

composition-density fluctuations. Furthermore, since the grain sizes are an order of magnitude larger than those reported in [11], we expect the scattering originated from grain boundaries in our samples to be much less than that in those nanocrystalline solids produced by inert-gas condensation. Following a theoretical calculation based on packing regular fourteen-faced tetrakaidecahedrons [14], a decrease from 48 to 13% in the intergranular volume fraction is expected for an increase in grain sizes from 5 to 20 nm. The intergranular volume fraction includes grain boundaries and triple junctions; in our case the latter would represent only 5%.

Therefore, the nature of the observed inhomogeneities is addressed in terms of the general two-phase model: Fe-rich regions in a matrix of different composition; no contribution from grain boundaries or voids (if present) is taken into account for this analysis. The integrated intensity or invariant Q is related to the mean density fluctuation $\langle\Delta\rho\rangle^2 = (\rho_1 - \rho_2)^2 c(1-c)$, where ρ_1, ρ_2 and c, $1-c$ are the electronic densities and volume fractions of phases 1 and 2, respectively, through the formula

$$Q = \int_0^\infty I(k)k^2\,\mathrm{d}k = 2\pi^2\langle\Delta\rho^2\rangle V \tag{1}$$

which is valid for particulate and non-particulate two-phase systems. V is the irradiated volume, which was kept fixed for all the samples studied. The integration was performed separately in three k-regions: using a triangular approximation for $k < k_0$, where k_0 is the first data point; by numerical integration for the measured scattering vector range; and using the analytical expression of the Porod k^{-4}-power law from the last data point to ∞. Explicit formulae can be found in the appendix of [15].

The Q-values obtained from integral (1) are shown in figure 4 as a function of Fe concentration y. The volume fraction of scatterers may be obtained from Q, if only one contrast is present. On the other hand, no Fe contamination from ball-milling tools is expected for Cu [16].

4. Discussion

In previous Mössbauer effect and XRD studies of the Fe_yCu_{1-y} ($0.141 \leqslant y \leqslant 0.45$) alloys, no signs of either α-Fe or γ-Fe were detected. The XRD patterns taken from samples which

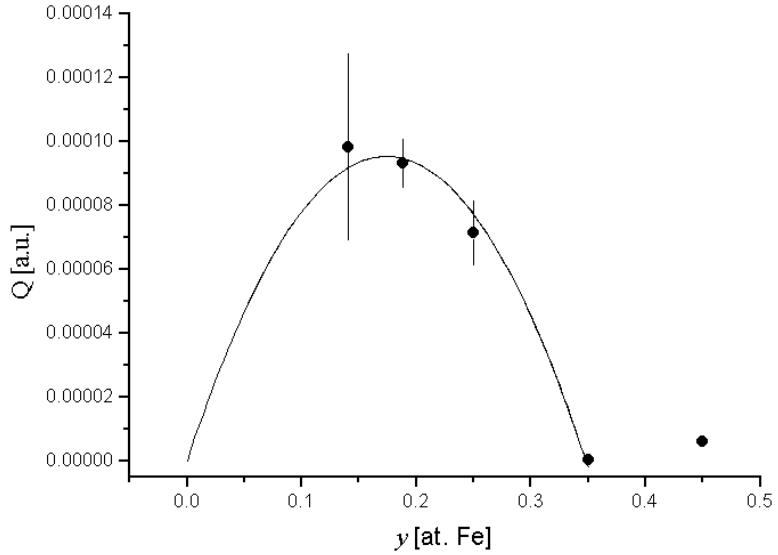

Figure 4. Integrated intensity (Q) versus iron concentration. The full curve corresponds to the best fit of the data with the two-phase model proposed.

have achieved the stationary state suggest a rather homogeneous solid solution: they only reveal the diffraction lines of fcc Cu, slightly shifted to lower angles, indicating increasing lattice parameter with y (maximum 0.371 ± 0.03 nm for $y = 0.45$), and show the typical line broadening originated from the strain and the small-grain-size effect. On the other hand, the GMR effect has been detected with a maximum effect at 0.2 at.% Fe [3], a fact which can only be explained by assuming the existence of magnetic clusters in a non-magnetic matrix. In agreement with the last observation, our SAXS results indicate that the alloys are inhomogeneous, with a distribution of inhomogeneity sizes ranging up to 12 nm. The main peak of the distribution is centred at 2 nm.

For the Fe–Cu system the alloying mechanism occurring upon grinding has been well established [2]. As grinding proceeds, the two metals quickly agglomerate and the particles are repeatedly flattened and welded by the colliding balls, leading to a lamellar-type structure which breaks down for further co-deformation into Fe needle-shape particles via multiple necking to rupture. This breaking process continues up to the nanometre scale, reaching a size for which Fe atoms may be dissolved in the Cu matrix.

Our SAXS data are in agreement with a particle-type structure and not with a lamellar-type structure for which a k^{-2}-power law is expected in the range of k preceding the Porod region [17].

Taking into account equation (1) and the fact that for the general two-phase model $\langle \Delta\rho \rangle^2 = c(1-c)(\rho_1 - \rho_2)^2$, we have attempted a qualitative description of how the matrix and scattering object composition must vary in order to account for the behaviour of the measured Q-values. To that end, mean compositions Cu_pFe_{1-p} (phase 1) and $Cu_{1-q}Fe_q$ (phase 2) for the scattering objects and matrix, respectively, were assumed and constrained to the nominal composition through $a_1(1-p) + a_2 q = y$, $a_1 p + a_2(1-q) = 1 - y$ and $a_1 + a_2 = 1$, where a_i is the fractional number of atoms in phase i. The volumes of the phases were taken as $V_1 = a_1((1-p)/n_{Fe} + p/n_{Cu})$ and $V_2 = a_2(q/n_{Fe} + (1-q)/n_{Cu})$, where n_{Fe}, n_{Cu} are the Fe and Cu atomic densities, respectively. The volume fraction

of phase 1 is $c = V_1/V_1 + V_2$ and that of phase 2 is equal to $1 - c$. For this case, $c(1-c) = (y-q)(1-p-y)/(1-q-p)^2$ (where the formula was simplified by assuming that $n_{Fe} \cong n_{Cu} = n$). Then, $(\rho_1 - \rho_2)^2 = (1-p-q)^2(Z_{Cu}n_{Cu} - Z_{Fe}n_{Fe})^2$, where the atomic scattering factors of Fe and Cu have been approximated by the corresponding atomic numbers Z_{Fe} and Z_{Cu} which is a good approximation for small-angle scattering. Finally, the expression $Q = 2\pi^2 V(y-q)(1-p-y)(Z_{Cu} - Z_{Fe})^2 n^2$ was obtained for the invariant. Then, the fitting function $D(y-q)(1-p-y)$ was used to describe the Q-dependence, in which p, q and D are fitting parameters to be determined. The parameter D includes the factor $2\pi^2 V(Z_{Cu} - Z_{Fe})^2 n^2$ and a normalizing factor, since the data are in arbitrary units. Figure 4 shows the best fit obtained with $D = 0.0032(2)$, $p = 0.652(6)$ and $q = 0.00(6)$, indicating that the scattering objects have a composition of about 0.35 at.%. Then, $Fe_{0.35}Cu_{0.65}$ phase is dispersed into a nearly pure Cu matrix. Roughly, this composition agrees with the value $p = 0.30$ suggested for $Fe_{0.6}Cu_{0.4}$ by Eckert *et al* [13]. The invariant was also analysed assuming a dependence of the phases on composition and no substantial improvement in the fitted results was obtained.

As mentioned above, some scattering from grain boundaries may be contributing to the measured signal. In order to separate these contributions from compositional inhomogeneities, an anomalous small-angle x-ray scattering (ASAXS) experiment would be needed. Such an experiment has been performed, for instance, for a Fe–Cu alloy quenched from a liquid with composition within the miscibility gap [18], and we may perform such an experiment on our samples in the future.

5. Conclusions

In summary, our SAXS results indicate that magnetoresistive fcc Fe_yCu_{1-y} alloys ($0.141 \leqslant y \leqslant 0.45$) produced after 75 h of ball milling are inhomogeneous at the nanometric scale with constant contrast arising from composition fluctuations inside nanocrystalline grains. Volumetric particle size distributions obtained assuming a spherical form factor indicate a 2 nm main size for the scattering objects. The two-phase analysis of the invariant Q suggests $Fe_{0.35}Cu_{0.65}$ scattering objects in a Cu matrix.

Acknowledgments

This research was supported by *CONICET* of República Argentina (through Programa TENAES) and *Fundaciones Vitae, Brasil/Antorchas, Argentina* (project N TC 059/97). The authors gratefully acknowledge G Kellerman for technical help at the LNLS SAXS beamline.

References

[1] Fecht H J 1998 *Nanomaterials, Synthesis, Properties and Applications* ed A S Edelstein and R C Cammarata (Bristol: Institute of Physics Publishing) p 96
[2] Yavari A R, Desré P J and Benameur T 1992 *Phys. Rev. Lett.* **68** 2235
[3] Uenishi K, Kobayashi K, Nasu S, Hatano H, Ishihara K and Shingu P H 1992 *Z. Metallk.* **83** 132
[4] Socolovsky L M, Sánchez F H, Shingu P H, Ishihara K, Otsuki A and Yasuna K 1998 *Hyperfine Interact.* C **3** 210
[5] Chien C L, Xiao J Q and Jiang J S 1993 *J. Appl. Phys.* **73** 5309
[6] Nakhimovitch N M 1941 *J. Phys. USSR* **5** 141
[7] Kellerman G, Vincentin F, Tamura E, Rocha M, Tolentino H, Barbosa L, Craievich A and Torriani I 1997 *J. Appl. Crystallogr.* **30** 1
[8] Boehme R F and Cargill G S 1984 *Polyimides* vol 1, ed K L Mittal (New York: Plenum)

[9] Svergun D I 1992 *J. Appl. Crystallogr.* **25** 495
[10] Roth M 1977 *J. Appl. Crystallogr.* **10** 172
Liu S and Moteff J 1978 *J. Appl. Crystallogr.* **11** 597
[11] Jorra E, Franz H, Peisl J, Wallner G, Petry W, Birringer R, Gleiter H and Haubold T 1989 *Phil. Mag.* B **60** 159
[12] Wagner W, Averback R S, Hahn H, Petry W and Widenmann A 1991 *J. Mater. Res.* **6** 2193
[13] Eckert J, Holzer J C and Johnson W L 1993 *J. Appl. Phys.* **73** 131
[14] Palumbo G, Thorpe S J and Aust K T 1990 *Scr. Metall.* **24** 1347
[15] Fernández van Raap M B, Regan M J and Bienenstock A 1995 *J. Non-Cryst. Solids* **191** 155
[16] Sánchez F H, Rodriguez Torres C E, Fernández van Raap M B and Mendoza Zélis L 1998 *Hyperfine Interact.* C **269–277** 113
[17] Porod G 1982 *Small-Angle X-ray Scattering* ed O Glatter and O Kratky (London: Academic) p 36
[18] Fratzl P, Yoshida Y, Vogl G and Haubold H G 1992 *Phys. Rev.* B **46** 11 323